



# Rapid ice aggregation process revealed through triple-wavelength Doppler spectra radar analysis

Andrew I. Barrett<sup>1,2</sup>, Christopher D. Westbrook<sup>1</sup>, John C. Nicol<sup>1</sup>, and Thorwald H. M. Stein<sup>1</sup>

<sup>1</sup>Department of Meteorology, University of Reading, Reading, RG6 6BB, UK

<sup>2</sup>Institute for Meteorology and Climate Research, Karlsruhe Institute of Technology, Karlsruhe, 76131, Germany

**Correspondence:** Andrew Barrett ([andrew.barrett@kit.edu](mailto:andrew.barrett@kit.edu))

## Abstract.

Rapid aggregation of ice particles has been identified by combining data from three co-located, vertically-pointing radars operating at different frequencies. A new technique has been developed that uses the Doppler spectra from these radars to retrieve the vertical profile of ice particle size distributions.

5 The ice particles grow rapidly from a maximum size of 0.75 mm to 5 mm while falling less than 500 m and in under 10 minutes. This rapid growth is shown to agree well with theoretical estimates of aggregation, with aggregation efficiency close to 1, and is inconsistent with other growth processes, e.g. growth by deposition, riming. The aggregation occurs in the middle of the cloud, and is not present throughout the entire lifetime of the cloud. However, the layer of rapid aggregation is very well defined, at a constant height, where the temperature is  $-15^{\circ}\text{C}$ , and lasts for at least 20 minutes (approximate horizontal  
10 distance: 24 km). Immediately above this layer, the radar Doppler spectra is bi-modal, which signals the formation of new small ice particles at that height. We suggest that these newly formed particles, at approximately  $-15^{\circ}\text{C}$ , grow dendritic arms, enabling them to easily interlock and accelerate the aggregation process. The estimated aggregation efficiency in the studied cloud is between 0.7 and 1, consistent with recent laboratory studies for dendrites at this temperature.

A newly developed method for retrieving the ice particle size distribution using the Doppler spectra allows these retrievals  
15 in a much larger fraction of the cloud than existing DWR methods. Through quantitative comparison of the Doppler spectra from the three radars we are able to estimate the ice particle size distribution at different heights in the cloud. Comparison of these size distributions with those calculated with more basic radar-derived values and more restrictive assumptions agree very well; however, the newly developed method allows size distribution retrieval in a larger fraction of the cloud because it allows us to isolate the signal from the larger (non-Rayleigh scattering) particles in the distribution and allows for deviation from the  
20 assumed shape of the distribution.

## 1 Introduction

Ice microphysical processes are an important part of cloud and precipitation formation; most surface precipitation begins as ice particles (Field and Heymsfield, 2015). However, numerical models, of either weather or climate, have difficulty accurately simulating ice cloud. For example, the CMIP5 models have regional cloud ice water paths that differ from observations by



factors of 2–10 (Li et al., 2012). This challenge is partly because observations of ice particles are sparse and because processes controlling the formation and evolution of ice particles, such as aggregation, are poorly understood and crudely parameterized in most models.

Measuring the number and size of ice particles within clouds is challenging. The two main methods, in-situ aircraft observations, and active remote sensing observations, both have their deficiencies. First, active remote sensing instruments, such as radar and lidar, are good at measuring the bulk scattering quantities, such as radar reflectivity. However, converting from these bulk quantities to cloud microphysical properties requires numerous assumptions. In contrast, aircraft observations measure the size and number of ice particles directly, but only within a small sample volume, at a single height at any given time, and only during sporadic case studies. Furthermore, ice particle size distributions have been shown to be biased as a result of shattering of ice particles on aircraft-mounted instrument inlets (Westbrook and Illingworth, 2009; Korolev et al., 2011).

Nevertheless, cloud microphysical observations and in particular particle size distributions are important for many applications. One important application is the better understanding of processes that occur within clouds. For example, size distributions measured from aircraft have been used to study aggregation in cirrus clouds (Field et al., 2006). Furthermore, the size distribution itself affects the relative importance of vapor deposition, riming and aggregation of ice particles. Another important application is to provide observations with which numerical models can be evaluated and their parameterizations improved.

In this paper, we present observations of rapid changes of the ice microphysical properties that apparently result from rapid aggregation of ice particles. These observations were made using three co-located, vertically pointing radars at different frequencies (3, 35, 94 GHz). We are able to retrieve the ice particle size and number concentration through comparison of the Doppler spectra returns from each of the three radars.

Analysis of the radar Doppler spectra has previously been performed for the onset of drizzle in stratiform clouds (Kollias et al., 2011a, b) and the application of multi-frequency Doppler spectra has been used to determine the rain size distribution (Tridon and Battaglia, 2015; Tridon et al., 2017). For the ice phase, the three different frequencies have been used simultaneously to categorize rimed and unrimed particles from the surface (Kneifel et al., 2011, 2015, 2016) and from aircraft-based radar observations (Kulie et al., 2014). However, this is the first attempt to retrieve the ice particle size distributions from multi-frequency Doppler spectra observations. These retrievals are then used to evaluate the microphysical processes active within the clouds.

The aggregation efficiency of ice particles ( $E_{\text{agg}}$ ; the probability that two colliding particles will stick together) has previously been found to depend on both the particle habit and the temperature at which the collisions occur; however, a large range of values have been reported. A laboratory study (Hosler and Hallgren, 1960) where small particles were drawn past a large stationary ice target showed a weak temperature dependence of  $E_{\text{agg}}$  with a broad peak around  $-12^{\circ}\text{C}$  and maximum values of 0.1–0.2. Connolly et al. (2012) used a 10-m tall cloud chamber containing large concentrations of small ice particles settling under gravity and reported a much sharper peak of  $E_{\text{agg}}$  around  $-15^{\circ}\text{C}$ , with values of 0.4–0.9, but values below 0.2 at all other temperatures. Hobbs et al. (1974) reported that both the maximum dimension of ice aggregates and the probability of seeing aggregates increased at around  $-15^{\circ}\text{C}$ , which was linked to the preferred formation of dendritic particles at this temperature. This is supported by other studies showing larger  $E_{\text{agg}}$  in the presence of dendritic particles. Mitchell et al. (2006) found



$E_{\text{agg}}$  of around 0.55 for clouds dominated by dendrites at cloud top, but much lower values around 0.07 when dendrites were not present. Low  $E_{\text{agg}}$  values of 0.09 were also found for tropical anvil clouds where dendritic particles were not present at temperatures of  $-3^{\circ}\text{C}$  to  $-11^{\circ}\text{C}$  (Field et al., 2006). In the early stage of aggregation, Moisseev et al. (2015) reported that the aggregates were made up of a small number of dendritic particles. These studies seem to suggest that dendrites, which typically form at around  $-15^{\circ}\text{C}$ , can significantly increase the aggregation efficiency because the dendritic branches interlock with other particles, whereas the aggregation efficiency is much lower when dendritic particles are not present. In this study, retrievals from radar observations will be used to estimate the aggregation efficiency and will be compared with the laboratory-derived values.

This paper is organised with an overview of the instruments and data in section 2, an overview of the case study in section 3 and details about the retrieval in section 4. Section 5 details the cloud properties retrieved and section 6 summarizes the evidence for aggregation, with conclusions drawn in section 7.

## 2 Data and Methods

We use data from three co-located radars at the Chilbolton Observatory in Hampshire, Southern England. The radars operate at frequencies of 3 GHz (9.75-cm wavelength, 25-m antenna,  $0.28^{\circ}$  beamwidth), 35 GHz (8.58-mm wavelength, 2.4-m antenna,  $0.25^{\circ}$  beamwidth) and 94 GHz (3.19-mm wavelength, 0.46-m antenna,  $0.5^{\circ}$  beamwidth). The 35- and 94-GHz cloud radars are situated immediately next to one another, whereas the 3-GHz radar is sited less than 50 m away (Fig. 1). The sampling of the three radars was synchronized to within 0.1 seconds and full pulse-to-pulse power and phase measurements were recorded. For the 3-GHz radar, Doppler spectra were calculated every second and incoherently averaged over 10 seconds. For the 35-GHz and 94-GHz cloud radars, spectra were calculated every 0.11 and 0.08 seconds respectively and again incoherently averaged over 10 seconds. Assuming typical wind speeds of 20  $\text{ms}^{-1}$  aloft, the averaged spectra correspond to a 200-m section of cloud. Ground clutter was removed from the spectra by masking returns with velocity near zero. Noise levels were estimated from measurements beyond the range of meteorological echoes ( $> 10$  km) and subtracted from the individual spectra prior to averaging. The data from each radar was interpolated onto common range and velocity grids (60-m range by  $0.0195 \text{ m s}^{-1}$  velocity).

Because of the large antenna, it is necessary to apply a near-field correction to the 3-GHz data at heights below about 6 km. This correction factor was derived by comparing 3-GHz reflectivity profiles against those measured by the 35-GHz instrument (which has a much smaller antenna) in a number of Rayleigh scattering ice clouds. The magnitude of the correction was 1 dB at 5 km, rising to 3 dB at 3 km.

### 2.1 Data quality, calibration and attenuation correction

To account for potentially imperfect calibration and attenuation by atmospheric gases and liquid water in the lower troposphere, the 35- and 94-GHz reflectivity is corrected relative to 3-GHz radar. The 3-GHz radar is absolutely calibrated to within 0.5 dB, using the method of Goddard et al. (1994). The radar reflectivity value from the cloud radars (35 and 94 GHz) was adjusted to



**Table 1.** A summary of the terminology used throughout this paper, where F denotes the radar frequency.

symbol	variable name	variable definition	units
$Z_F$	radar reflectivity	total radar cross sectional area of scatterers within the target volume	dBZ [ $Z = \text{mm}^6 \text{m}^{-3}$ ]
$\text{DWR}_{F_1/F_2}$	dual-wavelength ratio	$Z_{F_1} - Z_{F_2}$	dB
$sZ_F$	spectral reflectivity	radar reflectivity per Doppler-spectra velocity bin	dBX [ $X = \text{mm}^6 \text{m}^{-3} (\text{m s}^{-1})^{-1}$ ]
$s\text{DWR}_{F_1/F_2}$	spectral dual-wavelength ratio	$sZ_{F_1} - sZ_{F_2}$	dB

match the 3-GHz radar reflectivity in each profile so as to remove any calibration or attenuation offsets. The adjustment amount was estimated in regions where Rayleigh scattering was expected at all three wavelengths<sup>1</sup> and hence where the reflectivity should be the same from each radar. The adjustments made reduce the median difference in reflectivity ( $Z$ ) in the Rayleigh scattering areas to 0 dB. The same adjustment to  $Z$  (in dB) is made throughout the profile. A different correction is applied individually to each 10-second profile; the equivalent dB correction is also applied to the spectra within the profile.

The multi-wavelength approach allows us to measure the diameter of ice particles that are comparable in size to the shortest radar wavelength, or larger (e.g. Kneifel et al., 2015, 2016). For ice particles comparable in size to the radar wavelength, non-Rayleigh scattering becomes important. For suitably large particles, it becomes possible to size the particles based on the different radar returns at different wavelengths.

The Doppler spectra approach allows for retrievals of particle size and number concentration to be made separately on particles of distinct fall velocities. We can use the multi-wavelength approach to determine the particle size from the “spectral dual-wavelength ratio” (sDWR; i.e. the difference in reflectivity of particles within a small range of fall velocities), but can additionally separate the particles based on their fall velocity allowing us to retrieve the ice particle size distribution.

A correction to the velocities measured by the radar is also applied. Unfortunately, the three radars were not precisely vertically pointing for this case. The 3-GHz radar was pointing vertically, but after analyzing the data, the 35- and 94-GHz radars were determined to be off-zenith by approximately  $0.2^\circ$  and  $0.15^\circ$  respectively in opposing directions. This mis-pointing is small and likely does not result in a substantial mis-match in sample volume given the 10-second integration time. However, this small mis-pointing means that the radar detects a small component of the horizontal wind in addition to the fall velocities of the ice particles. Although the pointing angle error is small, the horizontal wind component detected is of the order of a few centimeters per second, which is sufficiently large to affect our comparison of the Doppler spectra from the three radars. Therefore, we have made a correction to the velocity measurements for the 35- and 94-GHz radars to ensure that the spectra are

<sup>1</sup>Based on an analysis of reflectivity differences, Rayleigh scattering is assumed where the 3-GHz reflectivity is below 5 dBZ and the absolute difference between the 3- and 94-GHz velocity measurements is less than  $0.025 \text{ m s}^{-1}$ . Measurements were also excluded where the 3-GHz reflectivity was less than  $-10 \text{ dBZ}$  to avoid effects of residual ground clutter.



well aligned and can be compared. This correction is important because even a small shift in velocity can substantially affect the estimates of sDWR. In practice, the correction applied is  $+0.0585 \text{ m s}^{-1}$  for the 35-GHz radar and  $-0.0390 \text{ m s}^{-1}$  for the 94-GHz radar throughout the cloud layer. This correction is imperfect; however, we do not have independent measurements of the horizontal wind speed with sufficient accuracy and high enough vertical resolution to make a reliable height-dependent  
5 correction. Radiosonde data and ECMWF model output shows that the horizontal wind speed was near-constant with height throughout the cloud layer on this day, and inspection of many individual Doppler spectra indicate that our simple correction aligns the spectra very well in this case (see Figure 4a,d,g).

To reduce the noise in the spectra, each individual spectrum has been smoothed in velocity space by averaging over a  $0.0585 \text{ m s}^{-1}$  window, which equates to three velocity bins.

10 We mask out regions where significant turbulence is present because the vertical air motions are large and vary on small time and space scales compared to the particle fall velocities that we are trying to measure. Near the cloud base, there is a layer of substantial turbulence caused by ice particles sublimating as they fall into drier air and leading to destabilisation of the atmosphere in this layer. In this turbulent layer, the implicit assumption that measurements at a specific velocity are of a single particle size is invalid and Rayleigh scattering is assumed where the 3-GHz reflectivity is between  $-10$  and  $+5 \text{ dBZ}$ .  
15 Hence, we identify regions where turbulence is altering the spectra, based on the contribution of turbulence to spectral width using O'Connor et al. (2005, eqns. 10–15). Points where the velocity variance from turbulence exceed a threshold value of  $10^{-3} \text{ m}^2 \text{ s}^{-2}$  are not considered when performing our retrievals. This threshold value was chosen such that all affected regions were suitably masked and that the width of the Doppler spectrum was determined by microphysical rather than turbulent contributions.

### 20 3 The case - 17 April 2014

Figure 2a shows the radar reflectivity measured at Chilbolton for the thick stratiform ice cloud observed on 17 April 2014. This cloud formed in north-westerly flow, ahead of a cold front. The surface cold front reached Chilbolton at about 1800 UTC. The front was not associated with any surface precipitation at Chilbolton, and only very light precipitation across some other parts of Southern England.

25 The cloud top height was approximately 9 km, where 35-GHz reflectivity values are around  $-15 \text{ dBZ}$ , and increase to  $19 \text{ dB}$  at approximately 4 km altitude, near cloud base. The temperature at cloud top was  $-45^\circ\text{C}$  and the freezing level was at about 2.7 km.

The evolution of the cloud reflectivity and the ratio of 35-GHz and 94-GHz reflectivity are shown in Figure 2. The same cloud was analysed in Stein et al. (2015), who also used the triple-frequency radar data to determine that the cloud contained  
30 primarily aggregate snowflakes, consistent with the Westbrook et al. (2006, 2008a) scattering model. We focus on the the time from 1545 to 1620 UTC, where there are dual wavelength ratios up to 8 dB below 4.5 km (Fig. 2b).



**Figure 1.** A photograph of the three co-located radars at the Chilbolton Observatory, Hampshire, England. From left to right: the 3-GHz CAMRa radar, 94-GHz radar and 35-GHz radar.

#### 4 Retrieving the ice particle size distribution

To retrieve the ice particle size distribution from the Doppler spectra at three wavelength, we use the method described below. The method is illustrated at three separate heights in Figure 4. At a given range gate we:

1. Calculate the spectral dual-wavelength ratio ( $sDWR = sZ_{35} - sZ_{94}$ ) between spectral reflectivity ( $sZ$ ) at 35 and 94 GHz (Fig. 4a,d,g).
2. Use a scattering model to convert the  $sDWR$  value to a particle size. We use the Westbrook et al. (2006, 2008a) scattering model, based on its good agreement with observational data for this case (Stein et al., 2015). Additionally, the scattering

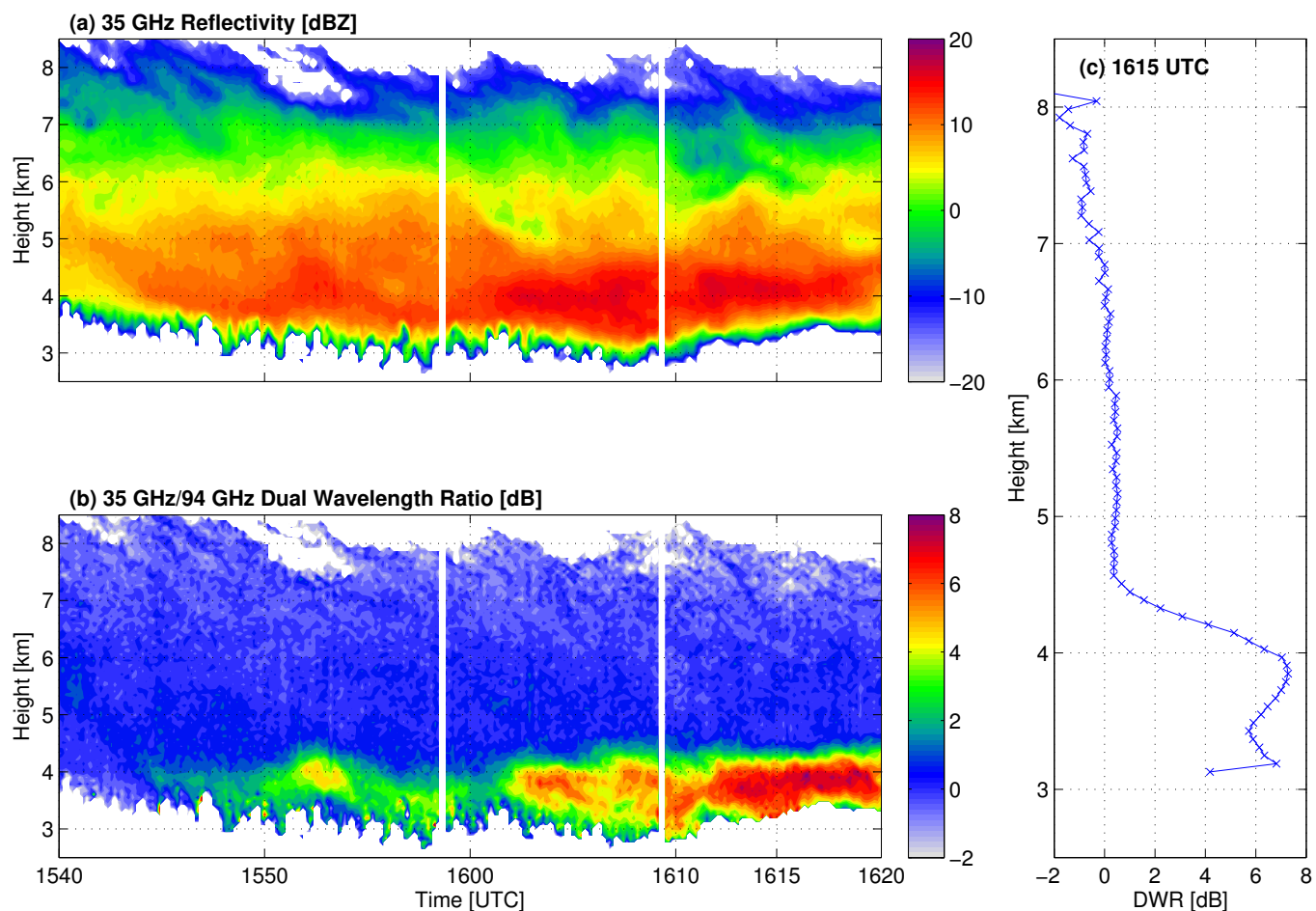


**Figure 2.** Overview of the cloud structure on 17 April 2014 showing the a) 35-GHz radar reflectivity and b) the ratio of 35-GHz reflectivity to 94-GHz reflectivity throughout the sampling period. c) The vertical profile of DWR at 1615 UTC.

model is used to calculate the reflectivity value for single particles of the retrieved size. (We assume the Brown and Francis (1995) mass-size relationship of  $m = 0.0185D^{1.9}$  for all ice particles).

3. Use the single-particle reflectivity calculated in the previous step and the total reflectivity measured by the radar to calculate the total number of particles of each size.
- 5 The size and number of ice particles within each velocity bin is now known (Fig. 4c,f,i).

Using this method we have determined the diameter of the ice particles  $D$  within each velocity bin, and also the particle velocity distribution  $dN/dV$  (where  $dN$  is the concentration of ice particles with velocity between  $V$  and  $V+dV$ ). We can convert  $dN/dV$  to the ice particle size distribution  $dN/dD$  (concentration of ice particles in a diameter bin, normalized by the bin width). To do so, we need to know the relationship between the velocity bin width  $dV$  and the diameter bin width  $dD$ . To

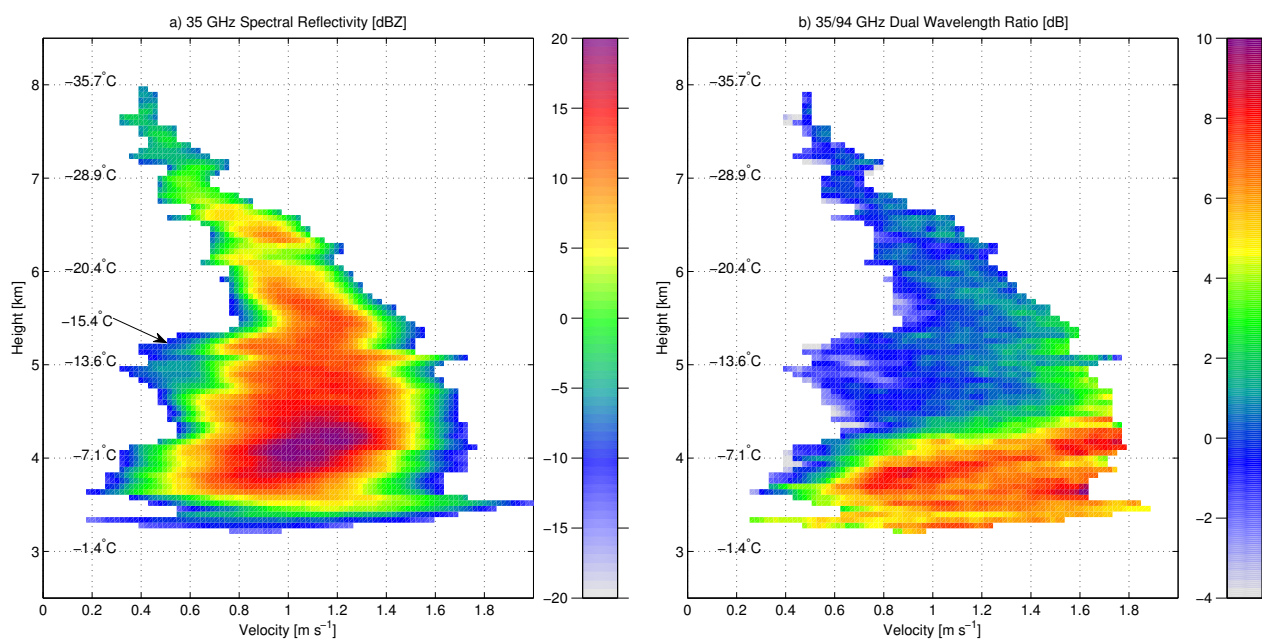


**Figure 3.** Height profile of a) spectral reflectivity at 35 GHz ( $sZ_{35}$ ) and b) spectral dual wavelength ratio ( $sDWR_{35/94}$ ) recorded at 1615 UTC. Temperatures from the ECMWF model at 1600 UTC are shown every 1 km and at 5.3 km where the small-particle mode is first evident.

determine this, we use a 300-m by 90-s window (5 range gates by 9 individual averaged spectra) centered on the current radar pixel and compute the optimal power-law fit to the velocity and diameter values, of the form  $V = cD^d$ . We use the differential of this power-law fit to compute the diameter bin width for each velocity bin. There is a relatively large sensitivity of the retrieved size distribution to the power-law fit, but only in terms of the absolute number concentration, rather than the diameter of the particles or the shape of the size distribution.

The retrieved size and number concentration of ice particles is only possible for particles larger than about 0.75 mm in diameter (corresponding to a  $sDWR_{35/94}$  of about 1 dB). For smaller particles the radar returns at all three frequencies are small and not easily distinguished from noise in the spectra. For particles larger than about 3 mm diameter, the  $sDWR_{35/94}$  saturates at about 8–9 dB as a result of the fractal geometry of the aggregates (see Stein et al., 2015). Therefore, where  $sDWR_{35/94}$  is larger than 6 dB, the diameter and number concentration are retrieved using  $sDWR_{3/94}$  using the same method as above.

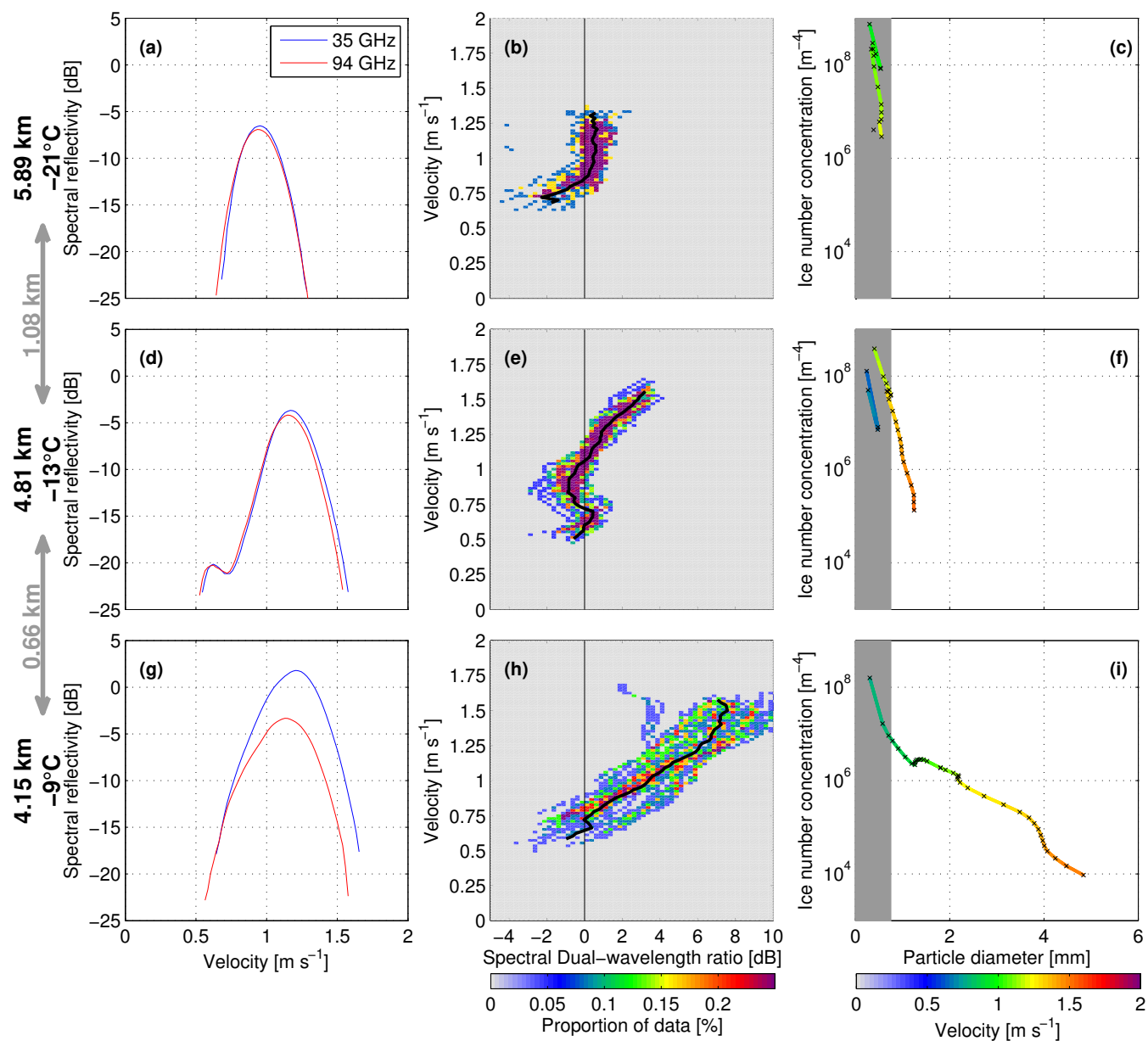


**Figure 4.** Illustration of the retrieval method and the retrieved size distribution at 3 heights at 1615 UTC. a-c are just above the layer of secondary ice nucleation, d-f are within that layer and g-i are below this layer, where the dual-wavelength differences are largest. a,d,g show the 35- and 94-GHz spectra at that height. b,e,h show the distribution of data points within a window around the central time (90-s by 300-m), with the black line denoting the median power difference for each velocity. c,f,i show the retrieved ice particle size distribution, with the color of the line related to the velocity of the data used to determine that data point. The gray shaded region marks particle diameters smaller than 0.75 mm, where there is no reliable information available to size the ice particles. The higher altitude plots are from earlier times to account for an approximately  $1 \text{ m s}^{-1}$  fall velocity of the ice particles.



## 5 Retrieved cloud properties and validation

Throughout most of the cloud, the 35/94-GHz dual-wavelength ratio ( $DWR_{35/94}$ ) is near zero ( $<1$  dB) (Fig 2b), implying that the ice particles are relatively small and are still in the Rayleigh scattering regime at 94 GHz (max diameter 0.75 mm).  $DWR$  only exceeds 2 dB after 1545 UTC and between 4.3 km and cloud base.

5 From 1600 to 1620 UTC, there is a sharp transition from  $DWR_{35/94} < 1$  dB at 4.5 km to peak  $DWR_{35/94}$  values at 4 km, with the maximum  $DWR_{35/94} = 8$  dB. The altitude of this sharp transition is consistent after 1602 UTC, with the largest  $DWR_{35/94}$  values being present after 1610 UTC. There is also evidence of this transition layer as early as 1545 UTC.

We focus on this period of substantial  $DWR_{35/94}$  and the rapid change in height to investigate the retrieved properties of the clouds and attempt to understand what causes the rapid change in cloud properties. Looking at the spectral reflectivity at each height (Fig. 3a) together with the spectral dual wavelength ratio (Fig. 3b) reveals the changes of the cloud properties with altitude. From these data, the origin of the large changes in the sharp transition can be identified. At 5.4 km, there is an increase in the signal coming from slow-falling particles ( $0.4\text{--}0.6\text{ ms}^{-1}$ ; Fig. 3a). At this height, only the fastest falling particles have  $sDWR_{35/94} > 1$  dB. At 4.5 km, the reflectivity and spectral reflectivity of the slow-falling particles has increased. The  $sDWR_{35/94}$  increases up to 8 dB for the fastest-falling particles, and by 4 km the increase in  $sDWR_{35/94}$  is seen for the majority of particles. Interestingly, the fall velocity of these particles does not increase as the particles grow larger and produce large  $sDWR_{35/94}$  values.

More detail can be seen by examining the Doppler spectra for the different radars at a few fixed heights in detail. The Doppler spectra measured at 5.89, 4.81 and 4.15 km (Fig. 4a,d,g) show three rather different shapes.

At 4.15 km, the spectra has only a single mode but throughout most of the velocity range  $sZ_{35}$  is much greater than  $sZ_{94}$ . The  $sDWR_{35/94}$  reaches 8 dB (Fig. 4h) and the largest particles are sized at 5 mm. The retrieved size distribution is approximately inverse exponential (Fig. 4i).

At 5.89 km (top row of Fig. 4), in contrast, the spectra for 35 and 94 GHz are very similar with a single peak and all  $sDWR_{35/94}$  values below 1 dB. The small  $sDWR_{35/94}$  values mean that it is not possible to reliably size the ice particles here, other than to say that they are all smaller than 0.75 mm.

25 About 1 km lower in the cloud, at 4.81 km (second row of Fig. 4), the mean velocity and reflectivity have both increased, but there is also a bi-modal structure to the spectra captured at both frequencies. This second mode is related to newly formed, small ice particles that are falling slower than the majority of older, larger ice particles. Furthermore, at 4.81 km, there are larger and faster-falling particles present than at 5.89 km. The largest  $sDWR_{35/94}$  values now approach 4 dB, and particles larger than 0.75 mm are present, with the largest retrieved diameter of 1.2 mm. The size distribution (Fig. 4f) of the reliably-sized particles (those larger than 0.75 mm and outside the gray region of the plot) is inverse exponential.

The consistent and narrow range of heights over which this rapid change in size occurs is just below the region where new particles are seen around 5.4 km and the Doppler spectra is bi-modal (Fig. 4a). These new particles fall slowly, which suggests that they are small and are nucleated at this level. These particles begin to fall faster as they grow in size. Particles forming around  $-15^{\circ}\text{C}$  would initially grow as dendrites (Takahashi et al., 1991). As these particles grow, the  $sDWR_{35/94}$



starts to increase for the larger (faster falling) particles, which we take to be aggregates. This increase in  $sDWR_{35/94}$  implies an acceleration of the aggregation process at this height.

The reduction of the size distribution slope between 4.81 km and 4.15 km remains consistent for at least 30 minutes from 1545 UTC onwards, but is not present earlier in the cloud. The observations shown in Fig. 4 are similar throughout this time period, which explains the sharp increase of DWR between 4.8 and 4.1 km (Fig. 2) during this time period.

### 5.1 Evolution and validation of retrieved size distributions

To evaluate how accurate the retrieved ice particle size distributions are, we would ideally like to compare against in-situ data. However, in-situ observations are not available for this case. Therefore, we evaluate the retrievals against other retrieval methods.

By fitting an inverse-exponential to the retrieved particle size distribution data from our Doppler spectra method, we can estimate the slope of the size distribution,  $\Lambda$  in  $dN/dD = N_0 \exp(-\Lambda D)$  (Fig. 5a). By means of verification, we also calculate the slope of a purely inverse-exponential size distribution fitted to match the  $DWR_{35/94}$  values only (Fig. 5b). There is excellent agreement between the two methods in the regions where the size distribution is broader and less steep. Fig. 5c shows a 3-minute average of  $\Lambda$ , which again shows the excellent agreement throughout the whole profile, particularly the height of the rapid change of  $\Lambda$  between 5 and 4 km. The only region of disagreement is just below 4 km, where the spectra method suggests even broader size distribution than the DWR method. This could be evidence that the inverse-exponential size distribution approximation in this region is not appropriate. However, both methods agree that there is a rapid increase in ice particle size occurring as they fall from 4.5 km to 3.6 km and a broadening of the ice particle size distribution. In the next section, we present evidence that this rapid change is occurring as a result of aggregation and not occurring through vapor deposition or riming.

The spectral method developed here is more sensitive to the presence of a few large particles than the DWR method. With the spectral method, the influence of a few non-Rayleigh scatterers can be seen in the spectra before the reflectivity of the individual scatterers is large enough to contribute significantly to the total reflectivity (which is a weighted average of  $sDWR$  over all particles). Therefore, the retrieved particle size distributions higher in the cloud are more reliable with the spectral method than the DWR method, because we are able to isolate the signal from the larger particles in the distribution. However, the spectral method is sensitive to noise in the spectra, and hence when the overall signal becomes weak, and the noise is therefore a more significant contributor, the retrieved particle size distributions are also noisy.

## 6 Evidence for rapid aggregation of dendrites

In this section we examine whether the changes in particle size and size distribution could be explained by processes other than aggregation. Specifically we address whether vapor deposition or riming could lead to the observed changes.

Ice particles grow from smaller than 0.75 mm in diameter ( $DWR < 1$  dB), above this transition layer, to larger than 5 mm by the time they reach 4 km (Figure 2c). Mean radar Doppler velocities just above this transition layer are 1–1.2 m s<sup>-1</sup>



(Figure 4d), indicating that on average ice particles will take 400–500 seconds to fall from 4.5 to 4 km, although the largest particles responsible for the high DWR values will fall faster than the average particle.

The growth of ice particles by vapor deposition cannot produce large ice particles sufficiently quickly to match our observations. Calculations using the vapor deposition growth equation from Pruppacher and Klett (1978) are presented to demonstrate this. The equations used were,

$$\frac{dm}{dt} = \frac{4\pi C SS_i F}{\left(\frac{L_s}{R_v T} - 1\right) \frac{L_s}{KT} + \frac{R_v T}{e_{si}(T)D}}, \quad (1)$$

$$m = 0.0185D^{1.9}, \quad (2)$$

where the rate of change of particle mass  $m$  with time  $t$  is a function of the ice particle capacitance  $C$  (assumed =  $D/4$  here, following Westbrook et al. (2008b), where  $D$  is the diameter), supersaturation with respect to ice  $SS_i$  and ventilation coefficient  $F$ . Terms on the denominator are the latent heat of sublimation  $L_s$ , the specific gas constant for vapor  $R_v$ , temperature  $T$ , thermal conductivity of air  $K$ , and saturated vapor pressure over ice  $e_{si}$ , (2) is the Brown and Francis (1995) mass-size relationship. These calculations, for a liquid-saturated atmosphere at  $-10^\circ\text{C}$ , show that typical ice particles (Brown and Francis, 1995) would, at their absolute fastest, take over 40 minutes (2534 seconds) to grow from 0.75 mm to 5 mm in diameter. Similarly, Fukuta and Takahashi (1999) calculate that it takes over 30 minutes to grow a particle of 3 mm through vapor deposition. We therefore can rule out pure vapor deposition as the source of the largest particles, which develop in less than 10 minutes.

Riming of the ice particles by collecting liquid water is another possible explanation; however, there is no evidence of significant supercooled liquid water present at this height. There were no strong backscatter returns in the lidar measurements (not shown) which would indicate the presence of liquid droplets, and the liquid water path measured by the microwave radiometer is below the noise level of the instrument (about  $20 \text{ g m}^{-2}$ ) throughout the observation period.

The sharp and consistent transition of cloud properties with height after 1545 UTC is therefore likely a result of aggregation. The first indication that aggregation is the most important process in this part of the cloud is the continual decrease of  $\Lambda$  (the slope of the ice particle size distribution) with height down from the top of the transition layer. This change with height indicates that there are more large particles and fewer small particles as the particle size distribution evolves, consistent with aggregation. In the case of vapor deposition or riming, one would expect the size of all particles to increase but the relative number of small and large particles would be mostly unchanged. Following Mitchell (1988), we calculate the expected change of  $\Lambda$  with height for several different values of aggregation efficiency ( $E_{\text{agg}}$ ). These calculations assume that aggregation is the only process affecting the evolution of the size distribution and that the ice-mass flux (“snowfall rate”) is constant with height. Using the retrieved size distribution properties at 4.5 km height as input, the expected change with height of  $\Lambda$  for  $E_{\text{agg}}$  values of 0.2, 0.7 and 1.0 are shown in Fig. 5c. The evolution of  $\Lambda$ , as calculated by either the Doppler spectra method or the simpler DWR method, both fall within the  $E_{\text{agg}} = 0.7$  and 1.0 curves. The value of 0.2, reported in Hosler and Hallgren (1960) cannot reproduce the observed broadening of the size distribution through this shallow layer of cloud, and leads to  $\Lambda$



being overestimated by almost an order of magnitude at 3.5 km. This value of  $E_{\text{agg}}$  is at the higher end of values reported in the literature. However, Connolly et al. (2012) found  $0.4 < E_{\text{agg}} < 0.9$  at  $-15^{\circ}\text{C}$ , whereas for all other temperatures sampled the best estimate was  $E_{\text{agg}} \leq 0.2$ . Similarly, Field et al. (2006) reported that  $E_{\text{agg}}$  values greater than unity were required for small particles for a good fit to observed aggregation within tropical cirrus anvils. Our results are consistent with the high values of  $E_{\text{agg}}$  of Connolly et al. (2012) at  $-15^{\circ}\text{C}$ , but do not support the  $E_{\text{agg}} < 0.2$  reported by Hosler and Hallgren (1960). This suggests that the free-fall experiments in the 10-m cloud chamber are more representative of the natural aggregation in the atmosphere than the stationary target experiments of Hosler and Hallgren (1960). Connolly et al. (2012) speculate that the higher  $E_{\text{agg}}$  at  $-15^{\circ}\text{C}$  is because the dendritic branches of the crystals are able to interlock and that this can increase  $E_{\text{agg}}$  by at least a factor of 3. Increased aggregation efficiency in the presence of dendritic crystals also agrees with observations by Hobbs et al. (1974).

## 7 Conclusions

We have shown that the use of radar Doppler spectra data from three co-located, vertically-pointing radars at frequencies of 3, 35 and 94 GHz can produce estimates of the ice particle size distribution and be used to identify and explore processes such as aggregation. Different radar reflectivity for different radar frequencies shows evidence that there are particles present that are large enough that they are no longer within the Rayleigh scattering regime. Using the Doppler spectra from the three radars, we can determine the size and number of these ice particles.

In the case presented in this paper, we identify a region where the 35 to 94 GHz dual-wavelength ratio (DWR) increases rapidly with decreasing height, indicative that large ice particles are forming quickly. We have ruled out vapor deposition as the cause of these large particles, because that process is too slow. Similarly the rapid growth is not a result of riming because there was no evidence of significant liquid water. We therefore argue that these large particles, up to 5 mm in diameter, are a result of aggregation. Our observations are consistent with theoretical calculations of ice particle size distribution evolution resulting from purely aggregation. In this case an aggregation efficiency of 0.7 to 1.0 fits the observations.

Aggregation as the cause of the rapid growth of ice particles is supported by the consistent and narrow range of heights over which this change occurs. The rapid aggregation occurs just below the region where the Doppler spectra is bi-modal, indicating the presence of small, newly-formed ice particles. It appears that the small ice particles forming at approximately 5.3 km ( $-15.4^{\circ}\text{C}$ ), and appearing clearly in the Doppler spectra at 4.8 km (Fig. 4d), grow into dendritic ice particles at temperatures around  $-15^{\circ}\text{C}$  and either aggregate with other similarly formed particles, or initiate aggregation with pre-existing ice particles falling through this layer. The aggregation initiated by these particles is then evident by the large particles present at 4.1 km, which could not have been formed by vapor deposition or riming.

These observations of rapid aggregation at temperatures around  $-15^{\circ}\text{C}$  add support to cloud chamber studies (Connolly et al., 2012; Hobbs et al., 1974), which also suggest that aggregation at around  $-15^{\circ}\text{C}$  is much more efficient than at other temperatures. The resulting changes to the ice particle size distribution through this aggregation process strongly affect many microphysical process rates (e.g. vapour deposition, sedimentation velocity, further aggregation) and therefore failure to capture

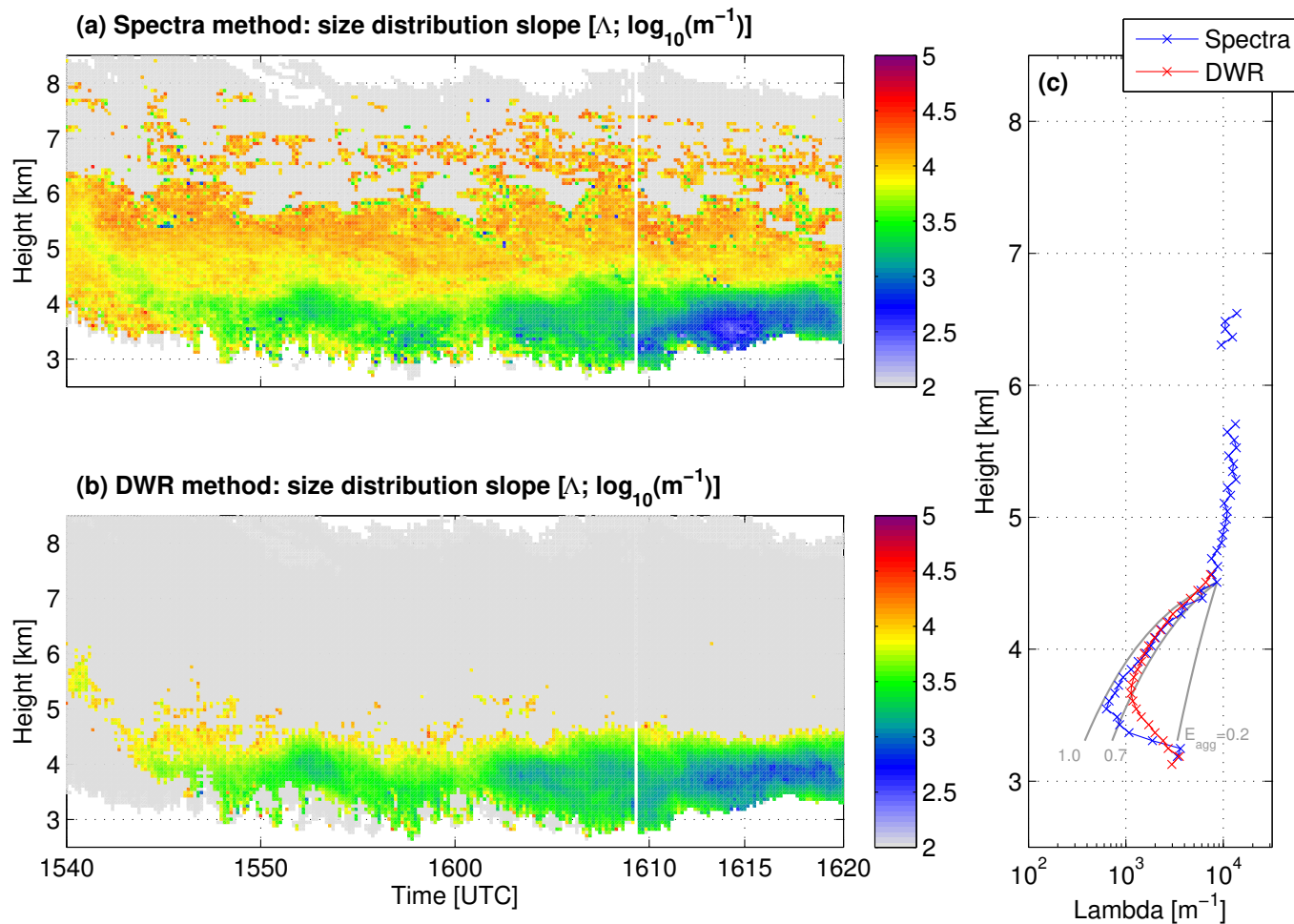


**Figure 5.** Time-height plots of  $\Lambda$ , the slope of the ice particle size distribution derived from the a) multi-wavelength Doppler spectra method and b) the dual-wavelength ratio (DWR) method. See text for details. Panel c) shows a profile of values averaged over 2 minutes centred on 1615 UTC. The grey lines show the expected changes in  $\Lambda$  for three different values of aggregation efficiency (1.0, 0.7, 0.2), assuming the ice particle size distribution at 4.5 km evolves due to aggregation alone.

these aggregation regions in models can lead to significantly errors in the simulated cloud fields. Barrett et al. (2017) showed that the assumed particle size distribution is the largest single sensitivity in the model physics for mixed-phase altocumulus clouds. The importance of correctly simulating the ice particle size distribution has been shown in several other studies (Pinto, 1998; Harrington et al., 1999; Field et al., 2005; Morrison and Pinto, 2006; Solomon et al., 2009). Therefore understanding and

5 correctly implementing the aggregation process in numerical models of cloud physics is important for the overall development of the cloud system.



This multi-wavelength Doppler spectra technique shows the ability to determine the size distribution of ice particles in large portions of ice clouds simultaneously. Previously, ice particle sizes have been determined using ice particle sizing instruments attached to aircraft, which suffer from two issues: small sample sizes and shattering of large ice particles on the instrument inlet, resulting in many small particles in the sample volume and leading to unreliable estimates of both large and small ice particle concentrations (Westbrook and Illingworth, 2009; Korolev et al., 2011). Therefore further studies of cloud microphysical structure and processes using this method are encouraged.

For the benefit of future studies, we give some advice here for achieving the best results. To achieve reliable, quantitative results from this method, the radars need to be very precisely pointed vertically. We find that mis-pointing by  $0.2^\circ$  is sufficient to resolve a non-negligible contribution from the horizontal wind in the Doppler spectra, which adds extra challenges to comparing the spectra from the three radars. Ideally the three radars should also have the same beamwidth; spectral broadening increases for wider beams and again makes comparing spectra from different radars more challenging. Despite these challenges, we have shown that this technique enables the generation of ice particle size distributions from remote sensing data, which will benefit the cloud microphysics community through both statistical sampling of clouds and aiding studies of individual processes, such as the aggregation process detailed in this paper. Further studies comparing the retrieved size distributions against data obtained from aircraft are currently being performed. Our current experimental setup means that we can only size particles larger than 0.75 mm. Particles smaller than this are in the Rayleigh scattering regime at all three wavelength and therefore their size cannot be determined. The addition of an extra shorted wavelength (e.g. at frequencies of 150 or 220 GHz, as advocated by Battaglia et al. (2014)), would enable sizing of particles down to approximately 0.45 or 0.3 mm (for 150 and 220 GHz respectively). Such observations would provide a unique opportunity for increasing our understanding of cloud microphysics, both statistically and through process studies as demonstrated in this paper.

*Acknowledgements.* This research was funded by the Natural Environment Research Council, grant NE/K012444/1. The radar data used in this paper can be accessed at the Centre for Environmental Data Archival ([www.ceda.ac.uk](http://www.ceda.ac.uk)) or by contacting the authors. We are grateful to the staff at the Chilbolton Facility for Atmospheric and Radio Research for operating and maintaining the radars and, in particular, Alan Doo, Allister Mallett, Chris Walden, John Bradford, and Darcy Ladd for their assistance in collecting the triple-wavelength measurements.



## References

- Barrett, A. I., Hogan, R. J., and Forbes, R. M.: Why are mixed-phase altocumulus clouds poorly predicted by large-scale models? Part I. Physical processes, *Journal of Geophysical Research: Atmospheres*, 122, 9903–9926, 2017.
- Battaglia, A., Westbrook, C. D., Kneifel, S., Kollias, P., Humpage, N., Löhnert, U., Tyynelä, J., and Petty, G. W.: G band atmospheric radars: new frontiers in cloud physics, *Atmospheric Measurement Techniques*, 7, 1527–1546, 2014.
- 5 Brown, P. R. A. and Francis, P. N.: Improved Measurements of the Ice Water Content in Cirrus Using a Total-Water Probe, *J. Atmos. Oceanic Technol.*, 12, 410–414, 1995.
- Connolly, P. J., Emersic, C., and Field, P. R.: A laboratory investigation into the aggregation efficiency of small ice crystals, *Atmos. Chem. Phys.*, 12, 2055–2076, 2012.
- 10 Field, P. and Heymsfield, A.: Importance of snow to global precipitation, *Geophysical Research Letters*, 42, 9512–9520, 2015.
- Field, P., Heymsfield, A., and Bansemer, A.: A test of ice self-collection kernels using aircraft data, *Journal of the atmospheric sciences*, 63, 651–666, 2006.
- Field, P. R., Hogan, R. J., Brown, P. R. A., Illingworth, A. J., Choullarton, T. W., and Cotton, R. J.: Parametrization of ice-particle size distributions for mid-latitude stratiform cloud, *Q. J. R. Meteorol. Soc.*, 131, 1997–2017, 2005.
- 15 Fukuta, N. and Takahashi, T.: The growth of atmospheric ice crystals: A summary of findings in vertical supercooled cloud tunnel studies, *Journal of the atmospheric sciences*, 56, 1963–1979, 1999.
- Goddard, J., Tan, J., and Thurai, M.: Technique for calibration of meteorological radars using differential phase, *Electronics Letters*, 30, 166–167, 1994.
- Harrington, J. Y., Reisin, T., Cotton, W. R., and Kreidenweis, S. M.: Cloud resolving simulations of Arctic stratus. Part II: Transition-season clouds, *Atmos. Res.*, 51, 45–75, 1999.
- 20 Hobbs, P. V., Chang, S., and Locatelli, J. D.: The dimensions and aggregation of ice crystals in natural clouds, *Journal of geophysical Research*, 79, 2199–2206, 1974.
- Hosler, C. and Hallgren, R.: The aggregation of small ice crystals, *Discussions of the Faraday Society*, 30, 200–207, 1960.
- Kneifel, S., Kulie, M., and Bennartz, R.: A triple-frequency approach to retrieve microphysical snowfall parameters, *Journal of Geophysical Research: Atmospheres*, 116, 2011.
- 25 Kneifel, S., Lerber, A., Tiira, J., Moisseev, D., Kollias, P., and Leinonen, J.: Observed relations between snowfall microphysics and triple-frequency radar measurements, *Journal of Geophysical Research: Atmospheres*, 120, 6034–6055, 2015.
- Kneifel, S., Kollias, P., Battaglia, A., Leinonen, J., Maahn, M., Kalesse, H., and Tridon, F.: First observations of triple-frequency radar Doppler spectra in snowfall: Interpretation and applications, *Geophysical Research Letters*, 43, 2225–2233, 2016.
- 30 Kollias, P., Rémillard, J., Luke, E., and Szyrmer, W.: Cloud radar Doppler spectra in drizzling stratiform clouds: 1. Forward modeling and remote sensing applications, *Journal of Geophysical Research: Atmospheres*, 116, 2011a.
- Kollias, P., Szyrmer, W., Rémillard, J., and Luke, E.: Cloud radar Doppler spectra in drizzling stratiform clouds: 2. Observations and microphysical modeling of drizzle evolution, *Journal of Geophysical Research: Atmospheres*, 116, 2011b.
- Korolev, A., Emery, E., Strapp, J., Cober, S., Isaac, G., Wasey, M., and Marcotte, D.: Small ice particles in tropospheric clouds: Fact or artifact? Airborne Icing Instrumentation Evaluation Experiment, *Bulletin of the American Meteorological Society*, 92, 967–973, 2011.
- 35 Kulie, M. S., Hiley, M. J., Bennartz, R., Kneifel, S., and Tanelli, S.: Triple-frequency radar reflectivity signatures of snow: Observations and comparisons with theoretical ice particle scattering models, *Journal of Applied Meteorology and Climatology*, 53, 1080–1098, 2014.



- Li, J.-L., Waliser, D., Chen, W.-T., Guan, B., Kubar, T., Stephens, G., Ma, H.-Y., Deng, M., Donner, L., Seman, C., et al.: An observationally based evaluation of cloud ice water in CMIP3 and CMIP5 GCMs and contemporary reanalyses using contemporary satellite data, *Journal of Geophysical Research: Atmospheres*, 117, 2012.
- Mitchell, D., Huggins, A., and Grubisic, V.: A new snow growth model with application to radar precipitation estimates, *Atmospheric research*, 82, 2–18, 2006.
- Mitchell, D. L.: Evolution of Snow-Size Spectra in Cyclonic Storms. Part I: Snow Growth by Vapor Deposition and Aggregation, *J. Atmos. Sci.*, 45, 3431–3451, 1988.
- Moisseev, D. N., Lautaportti, S., Tyynela, J., and Lim, S.: Dual-polarization radar signatures in snowstorms: Role of snowflake aggregation, *Journal of Geophysical Research: Atmospheres*, 120, 12 644–12 655, 2015.
- Morrison, H. and Pinto, J.: Intercomparison of bulk cloud microphysics schemes in mesoscale simulations of springtime Arctic mixed-phase stratiform clouds, *Mon. Wea. Rev.*, 134, 1880–1900, 2006.
- O'Connor, E. J., Hogan, R. J., and Illingworth, A. J.: Retrieving stratocumulus drizzle parameters using Doppler radar and lidar, *Journal of Applied Meteorology*, 44, 14–27, 2005.
- Pinto, J. O.: Autumnal mixed-phase cloudy boundary layers in the arctic, *J. Atmos. Sci.*, 55, 2016–2038, 1998.
- Pruppacher, H. R. and Klett, J. D.: *Microphysics of clouds and precipitation*, D. Reidel Publishing Company, Boston, USA, 1978.
- Solomon, A., Morrison, H., Persson, O., Shupe, M. D., and Bao, J.-W.: Investigation of microphysical parameterizations of snow and ice in Arctic clouds during M-PACE through model-observation comparisons, *Mon. Wea. Rev.*, 137, 3110–3128, 2009.
- Stein, T. H., Westbrook, C. D., and Nicol, J.: Fractal geometry of aggregate snowflakes revealed by triple-wavelength radar measurements, *Geophys. Res. Lett.*, 42, 176–183, 2015.
- Takahashi, T., Endoh, T., Wakahama, G., and Fukuta, N.: Vapor diffusional growth of free-falling snow crystals between -3 and -23 C, *Journal of the Meteorological Society of Japan. Ser. II*, 69, 15–30, 1991.
- Tridon, F. and Battaglia, A.: Dual-frequency radar Doppler spectral retrieval of rain drop size distributions and entangled dynamics variables, *Journal of Geophysical Research: Atmospheres*, 120, 5585–5601, 2015.
- Tridon, F., Battaglia, A., Luke, E., and Kollias, P.: Rain retrieval from dual-frequency radar Doppler spectra: validation and potential for a midlatitude precipitating case-study, *Quarterly Journal of the Royal Meteorological Society*, 143, 1364–1380, 2017.
- Westbrook, C., Ball, R., and Field, P.: Radar scattering by aggregate snowflakes, *Quarterly Journal of the Royal Meteorological Society*, 132, 897–914, 2006.
- Westbrook, C., Ball, R., and Field, P.: Corrigendum: Radar scattering by aggregate snowflakes, *Quarterly Journal of the Royal Meteorological Society*, 134, 547–548, 2008a.
- Westbrook, C. D. and Illingworth, A. J.: Testing the influence of small crystals on ice size spectra using Doppler lidar observations, *Geophys. Res. Lett.*, 36, L12 810, 2009.
- Westbrook, C. D., Hogan, R. J., and Illingworth, A. J.: The Capacitance of Pristine Ice Crystals and Aggregate Snowflakes, *J. Atmos. Sci.*, 65, 206–219, 2008b.